MATHEMATICAL MODELLING OF PROCESSES OF RADIOLYSIS OF WATER, HEXANE AND WATER-HEXANE MIXTURE

A. A. Garibov, K. Eyubov, T. Agaev, G. Akhmedli

Institute of Radiation Problems of Azerbaijan National Academy of Sciences, Baku, Azerbaijan

Introduction

In order to explain the obtained experimental data and to reveal possible mechanisms of the reactions upon radiolysis of water, hexane and water-hexane mixture modeling of the processes occurring in these systems has been carried out. In this modeling the following factors were taken into account: dose rate, volume of the irradiated system, time of irradiation, concentrations of components, constants of the reactions rates, etc. Modeling of the process kinetics has been made with computer program GEPASI 3 for the Windows operating system. Description of this program is given in [1,2]. Constants of the reactions rates are taken from [3-9].

The main purpose of the modeling is to study the processes occurring in the water-hexane mixture upon γ-radiolysis. However, for comparison with the literature, separate radiolysis separately of liquid water and hexane was first modeled. In the case of liquid water rate constants from [3], [7], [9] as well as our own experimental data were used:

Dose rate-1,42 Gy/s.

Volume of ampoules-0,5 ml.

Time of irradiation-from 1 to 20 hr.

The reactions and rate constants of the reactions taken from [3] are given below:

Number of reaction	Reaction	K_1-constant of direct reaction, (l/mole·s)	K_2-constant of reverse reaction, (l/mole·s)
1	$2e_{aq} \rightarrow H_2 + 2OH^-$	$4{,}97 \cdot 10^9$	
2	$e_{aq} + H \rightarrow H_2 + OH^-$	$1{,}89 \cdot 10^{10}$	
3	$e_{aq} + OH \rightarrow OH^-$	$3 \cdot 10^{10}$	
4	$e_{aq} + O \rightarrow 2\ OH^-$	$2{,}2 \cdot 10^{10}$	
5	$e_{aq} + HO_2 \rightarrow HO_2^-$	$2 \cdot 10^{10}$	
6	$e_{aq} + O_2^- \rightarrow OH^- + HO_2^-$	$1{,}3 \cdot 10^{10}$	
7	$e_{aq} + H_2O_2 \rightarrow OH^- + OH$	$1{,}2 \cdot 10^{10}$	
8	$e_{aq} + HO_2^- \rightarrow OH^- + O^-$	$3{,}5 \cdot 10^9$	
9	$e_{aq} + O_2 \rightarrow O_2^-$	$1{,}8 \cdot 10^{10}$	
10	$e_{aq} + H^+ \rightarrow H$	$2{,}3 \cdot 10^{10}$	
11	$e_{aq} + H_2O \rightarrow OH^- + H$	19	
12	$2H \rightarrow H_2$	$7{,}8 \cdot 10^9$	
13	$H + OH \rightarrow H_2O$	$2{,}5 \cdot 10^{10}$	
14	$H + HO_2 \rightarrow H_2O_2$	$2 \cdot 10^{10}$	
15	$H + O_2^- \rightarrow HO_2^-$	$2 \cdot 10^{10}$	
16	$H_2O_2 + H \rightarrow OH + H_2O$	$8{,}42 \cdot 10^6$	
17	$O_2 + H \rightarrow HO_2$	$2{,}1 \cdot 10^{10}$	
18	$OH^- + H \rightarrow H_2O^-$	$2{,}2 \cdot 10^7$	

19	$2\ OH \leftrightarrow H_2O_2$	$5{,}5\cdot10^{9}$	$1{,}33\cdot10^{-7}$
20	$OH + O^{-} \rightarrow HO_2^{-}$	$2\cdot10^{10}$	
21	$OH + HO_2 \rightarrow O_2 + H_2O$	$6{,}3\cdot10^{9}$	
22	$OH + O_2^{-} \rightarrow O_2 + OH^{-}$	$8{,}2\cdot10^{9}$	
23	$H_2O_2 + OH \rightarrow HO_2 + H_2O$	$4{,}06\cdot10^{7}$	
24	$OH + HO_2^{-} \rightarrow OH^{-} + HO_2$	$7{,}5\cdot10^{7}$	
25	$H_2 + OH \rightarrow H + H_2O$	$3{,}8\cdot10^{7}$	
26	$OH^{-} + OH \leftrightarrow O^{-} + H_2O$	$1{,}2\cdot10^{10}$	$1{,}75\cdot10^{6}$
27	$2\ O^{-} \rightarrow OH^{-} + HO_2^{-}$	$1\cdot10^{9}$	
28	$O_2^{-} + O^{-} \rightarrow O_2 + 2\ OH^{-}$	$6\cdot10^{8}$	
29	$H_2O_2 + O^{-} \rightarrow O_2^{-} + H_2O$	$5\cdot10^{8}$	
30	$O^{-} + HO_2^{-} \rightarrow OH^{-} + O_2^{-}$	$4\cdot10^{8}$	
31	$H_2 + O^{-} \rightarrow OH^{-} + H$	$8\cdot10^{7}$	
32	$2\ HO_2 \rightarrow H_2O_2 + O_2$	$8{,}3\cdot10^{5}$	
33	$HO_2 + H_2O_2 \rightarrow O_2 + OH + H_2O$	0,2	
34	$O_2^{-} + HO_2 \rightarrow O_2 + HO_2^{-}$	$9{,}7\cdot10^{7}$	
35	$HO_2 \leftrightarrow H^{+} + O_2^{-}$	$7{,}5\cdot10^{5}$	$5{,}1\cdot10^{10}$
36	$2\ O_2^{-} \rightarrow H_2O_2 + O_2 + 2\ OH^{-}$	0,3	
37	$H_2O_2 + O_2^{-} \rightarrow O_2 + OH^{-} + OH$	0,13	
38	$O_2^{-} + HO_2^{-} \rightarrow O_2 + OH^{-} + O^{-}$	0,13	
39	$H_2O_2 + OH^{-} \leftrightarrow HO_2^{-} + H_2O$	$1\cdot10^{10}$	$1{,}13\cdot10^{6}$
40	$H^{+} + HO_2^{-} \rightarrow H_2O_2$	$2\cdot10^{10}$	
41	$H^{+} + OH^{-} \leftrightarrow H_2O$	$1{,}4\cdot10^{11}$	$2{,}52\cdot10^{-5}$
42	$O_2 + O^{-} \leftrightarrow O_3^{-}$	$3\cdot10^{9}$	300
43	$O^{-} + O_3^{-} \rightarrow 2\ O_2^{-}$	$7\cdot10^{9}$	
44	$H_2O_2 + O_3^{-} \rightarrow O_2 + O_2^{-} + H_2O$	$1{,}6\cdot10^{6}$	
45	$HO_2^{-} + O_3^{-} \rightarrow O_2 + OH^{-} + O_2^{-}$	$8{,}9\cdot10^{5}$	
46	$H_2 + O_3^{-} \rightarrow O_2 + OH^{-} + H$	$2{,}5\cdot10^{5}$	
47	$H^{+} + O^{-} \rightarrow OH$	$1\cdot10^{10}$	
48	$OH^{-} + HO_2 \rightarrow O_2^{-} + H_2O$	$1\cdot10^{10}$	

In the modeling the values of the particles yields given in [3] were also used:

Particle	G, particles/100eV
H_2O^{-}	2,7
H	0,6
H_2	0,45
OH	2,7
H_2O_2	0,7
O_2-	0,02
H^{+}	3,42
OH^{-}	0,7

Based on these data we have built several graphs and then carried out their comparison with the graphs given in literature, in particular, in [3] and [4].

Sufficient coincidence is observed which may serve as an evidence of correctness of the selected scheme and the used program.

In the case of hexane the rate constants of the reactions from [4-6], [8] were used and the experimental data remained as in the case of liquid water.

The reactions and the rate constants of the reactions taken from [4], [5] and [6] are given below:

Number of reaction	Reaction	K_1-constant of direct reaction, (l/mole·s)	K_2-constant of reverse reaction, (l/mole·s)
1	$C_6H_{14}^+ + e \rightarrow C_6H_{14}^*$	$3\cdot10^9$	
2	$C_6H_{14}^* \rightarrow C_6H_{13}^\bullet + H$	$8\cdot10^{-4}$	
3	$C_6H_{14}^* \rightarrow C_6H_{12} + H_2$	$4\cdot10^{-4}$	
4	$C_6H_{14} + H \rightarrow C_6H_{13}^\bullet + H_2$	$1{,}5\cdot10^8$	
5	$C_6H_{13}^\bullet + C_6H_{13}^\bullet \rightarrow C_6H_{12} + C_6H_{14}$	$1\cdot10^{10}$	
6	$C_6H_{14}^* \rightarrow CH_3^\bullet + C_5H_{11}^\bullet$	$2{,}7\cdot10^{-5}$	
7	$C_6H_{14}^* \rightarrow C_2H_5^\bullet + C_4H_9^\bullet$	$4\cdot10^{-6}$	
8	$C_6H_{14}^* \rightarrow C_3H_7^\bullet + C_3H_7^\bullet$	$6\cdot10^{-3}$	
9	$C_2H_5^\bullet + C_2H_5^\bullet \rightarrow C_4H_{10}$	$1\cdot10^{10}$	
10	$C_3H_7^\bullet + C_3H_7^\bullet \rightarrow C_3H_8 + C_3H_6$	$1\cdot10^{10}$	
11	$C_2H_6 + H \rightarrow C_2H_5^\bullet + H_2$	$1\cdot10^4$	
12	$CH_4 + H \rightarrow CH_3^\bullet + H_2$	$1\cdot10^4$	
13	$C_3H_8 + H \rightarrow C_3H_7^\bullet + H_2$	$1\cdot10^4$	
14	$C_4H_{10} + H \rightarrow C_4H_9^\bullet + H_2$	$1\cdot10^4$	
15	$C_5H_{12} + H \rightarrow C_5H_{11}^\bullet + H_2$	$1\cdot10^4$	
16	$CH_3^\bullet + CH_3^\bullet \rightarrow C_2H_6$	$1\cdot10^{10}$	
17	$CH_3^\bullet + H \rightarrow CH_4$	$2{,}3\cdot10^9$	
18	$C_2H_5^\bullet + H \rightarrow C_2H_6$	$3\cdot10^9$	
19	$C_3H_7^\bullet + H \rightarrow C_3H_8$	$8\cdot10^9$	
20	$C_4H_9^\bullet + H \rightarrow C_4H_{10}$	$5{,}2\cdot10^9$	
21	$C_5H_{11}^\bullet + H \rightarrow C_5H_{12}$	$5\cdot10^9$	
22	$C_6H_{13}^\bullet + H \rightarrow C_6H_{14}$	$5{,}5\cdot10^9$	
23	$CH_3^+ + CH_4 \rightarrow C_2H_5^+ + H_2$	$6\cdot10^{11}$	
24	$CH_4^+ + CH_4 \rightarrow CH_5^+ + CH_3^\bullet$	$7{,}6\cdot10^{11}$	
25	$C_2H_4^+ + C_2H_4 \rightarrow C_4H_8^+$	$1{,}2\cdot10^{11}$	
26	$C_2H_4^+ + C_2H_4 \rightarrow C_4H_7^+ + H$	$9\cdot10^{10}$	
27	$C_2H_6 + C_2H_6^+ \rightarrow C_4H_{10}^+ + H_2$	$2{,}4\cdot10^9$	
28	$C_2H_6 + C_2H_6^+ \rightarrow C_4H_9^+ + H_2 + H$	$6\cdot10^9$	

In the modelling the values of the particles yields given in [4] were also used:

Particle	G, particle/100eV
CH_3	0,7
C_2H_5	0,3
C_3H_7	0,3
C_4H_9	0,27
C_6H_{13}	4,1
e	0,12
H_2	5
CH_4	0,18
C_2H_6	0,42
C_3H_8	0,41
C_3H_6	0,19
C_4H_{10}	0,35
C_5H_{12}	0,1
C_6H_{12}	0,86
C_2H_4	0,25
C_4H_8	0,14
$C_6H_{14}^+$	0,12

Based on these data we have built kinetic curves for H_2, CH_4, $\sum C_2=[C_2H_6] + [C_2H_4]$, $\sum C_3=[C_3H_8] + [C_3H_6]$, $\sum C_4=[C_4H_{10}] + [C_4H_8]$ and $\sum C_5=[C_5H_{12}]$. In these graphs, along the ordinate axis the amount of molecules of a given substance is set while along the abscissa axis time in hours is shown (Fig.1-4)

According to these curves the rates of accumulation of radiolysis products and their radiation-chemical yields were calculated. The results also coincide with the data given in literature, for example, in [4].

Below, the values of particle accumulation rate W and yield G are given which were obtained upon radiolysis of hexane at the dose rate of 1,42 Gy/s

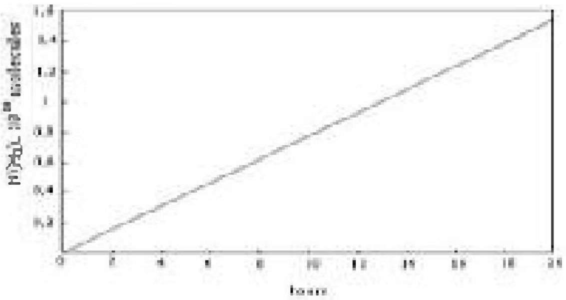

Fig 1. Kinetics of molecular hydrogen accumulation upon radiolysis of hexane at T=300K and dose rate of 1,42 Gy/s.

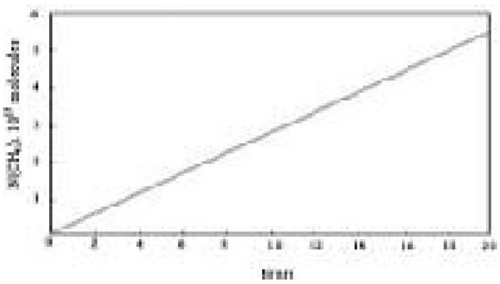

Fig 2. Kinetics of methane accumulation upon radiolysis of hexane at T=300K and dose rate of 1,42 Gy/s

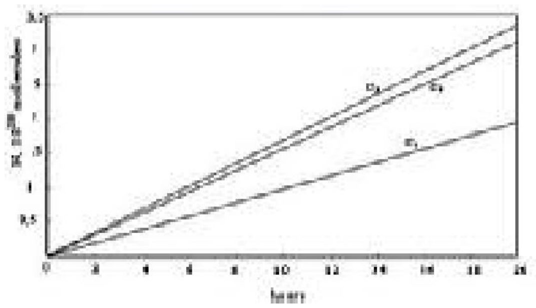

Fig 3. Kinetics of ethane, propane and buthane accumulation upon radiolysis of hexane at T=300K and dose rate of 1,42 Gy/s.

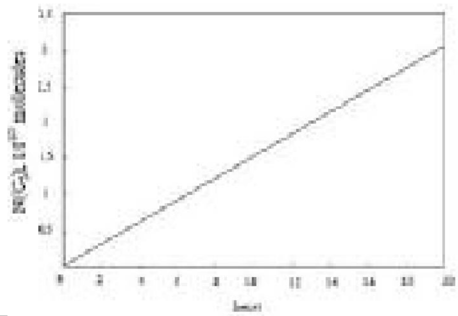

Fig 4. Kinetics of pentane accumulation upon radiolysis of hexane at T=300K and dose rate of 1,42 Gy/s.

Products of radiolysis	H_2	CH_4	C_2H_6	C_3H_8	C_4H_{10}	C_5H_{12}
W($\cdot$ 10^{14}), molecules/s	3	0,12	0,56	0,57	0,3	0,06
G, molecules/100eV	3,4	0,14	0,6	0,6	0,34	0,07

Modeling of radiolysis of water-hexane mixture has been carried out taking into consideration slight solubility of water in hexane and vice versa. For this reason it was assumed that radiolysis of this system is similar to the radiolysis of each of the components in separate. However, taking into account a possibility of diffusion of the radiolysis primary products from one phase into another, several new reactions with the respective rate constants [8] were added to the above-indicated reactions:

Number of reaction	Reaction	K-constant of direct reaction, (l/mole·s)
1	$C_6H_{14} + OH \rightarrow C_6H_{13}^{\bullet} + H_2O$	$1{,}37\cdot10^9$
2	$C_5H_{12} + OH \rightarrow C_5H_{11}^{\bullet} + H_2O$	$1{,}63\cdot10^9$
3	$C_4H_{10} + OH \rightarrow C_4H_9^{\bullet} + H_2O$	$1{,}8\cdot10^9$
4	$C_3H_8 + OH \rightarrow C_3H_7^{\bullet} + H_2O$	$2{,}5\cdot10^9$
5	$C_2H_6 + OH \rightarrow C_2H_5^{\bullet} + H_2O$	$2\cdot10^9$
6	$CH_4 + OH \rightarrow CH_3^{\bullet} + H_2O$	$1{,}5\cdot10^9$

Modeling was performed for the mixture of the following percentage content of the components: 50% C_6H_{14} + 50% H_2O, which in the experiment corresponded to the following volume ratio of the components: 0,2ml C_6H_{14} + 0,2ml H_2O. The kinetic curves were built for H_2, CH_4, $\sum C_2=[C_2H_6] + [C_2H_4]$, $\sum C_3=[C_3H_8] + [C_3H_6]$, $\sum C_4=[C_4H_{10}] + [C_4H_8]$ and $\sum C_5=[C_5H_{12}]$, where along the ordinate axis the number of molecules of a given substance and along the abscissa axis time in hours have been set. Our experimental data are shown as dotted curves in these graphs (Fig. 5-9):

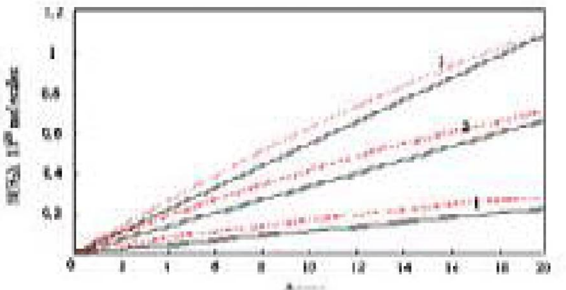

Fig 5. Kinetics of molecular hydrogen accumulation upon radiolysis of the water-hexane mixture at dose rate of 0,9Gy/s and of various ratios of the components:

1- C_6H_{14}/H_2O = 0.05ml/0.45ml
2- C_6H_{14}/H_2O = 0.15ml/0.35ml
3- C_6H_{14}/H_2O = 0.25ml/0.25ml

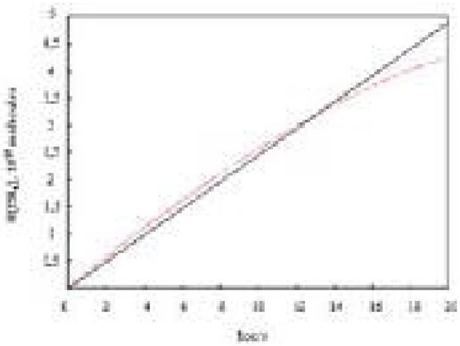

Fig 6. Kinetics of methane accumulation upon radiolysis of water-hexane mixture at T=300K and dose rate of 0,9 Gy/s.

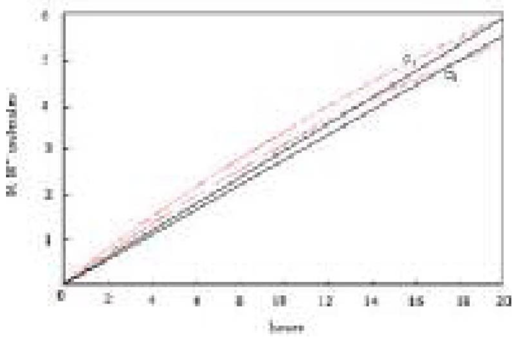

Fig 7. Kinetics of ethane and propane accumulation upon radiolysis of water-hexane mixture at T=300K and dose rate of 0,9 Gy/s.

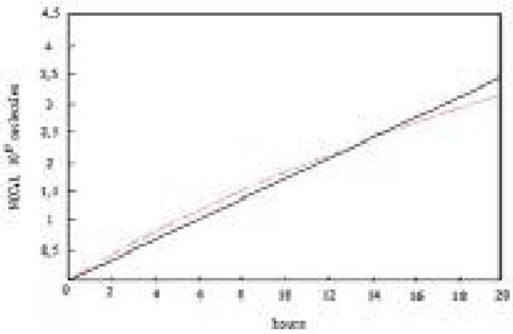

Fig 8. Kinetics of buthane accumulation upon radiolysis of water-hexane mixture at T=300K and dose rate of 0,9 Gy/s.

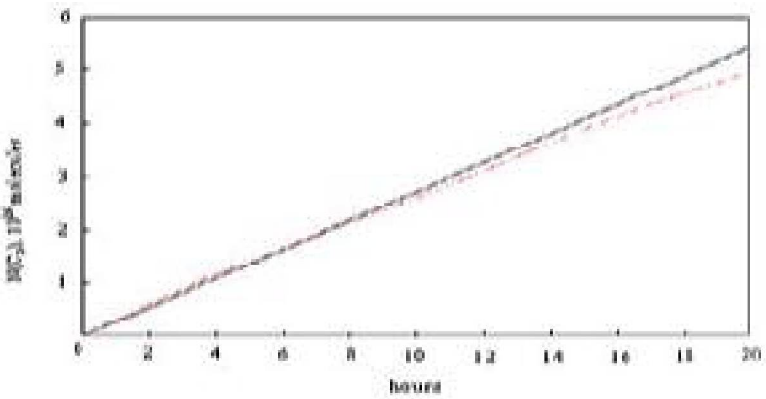

Fig 9. Kinetics of pentane accumulation upon radiolysis of water-hexane mixture at T=300K and dose rate of 0,9 Gy/s.

Based on these values of rates of particle accumulation W and their yield G have been calculated. The obtained data were compared with the experimental data at the same volume ratio of components, which correspond to dotted lines.

The comparison shows quite a good coincidence of the results that may serve as an evidence of correctness of the assumptions made. The result of modeling of radiolysis of the mixture C_6H_{14} + H_2O dose rate of 0,9 Gy/s is given below:

Products of radiolysis	CH_4	C_2H_6	C_3H_8	C_4H_{10}	C_5H_{12}
W(· 10^{13}), molecules/s	0,7	1,12	1,12	0,56	0,14
G, molecules/100eV	0,13	0,2	0,2	0,1	0,025

Modelling was separately made for kinetics of hydrogen formation upon radiolysis of C_6H_{14} + H_2O mixture of the above-shown percentage ratio of the components at dose rate of 1,42 Gy/s:

Products of radiolysis	H_2
W(· 10^{14}), molecules/s	2,8
G, molecules/100eV	3,3

References

1. Mendes P. GEPASI: A Software Package for Modelling the Dynamics, Steady States and Control of Biochemical and Other Systems. Comput. Applic. Biosci. 9, 1993, p.563-571.
2. Mendes P. Biochemistry by Numbers: Simulation of Biochemical Pathways with GEPASI 3. Trends Biochem. Sci. 22, 1997, p.361-363.
3. Bugayenko V., Byakov V. Quantitative Model of Radiolysis of Liquid Water and Diluted Aqueous Solutions of Hydrogen, Oxygen and Hydrogen Peroxide. I. Model Formulation // Preprints of Institute of Theoretical and Experimental Physics. 1991, №74-91. 24p.
4. Pikaev A. Modern Radiation Chemistry. Radiolysis of Gases and Liquids. Moscow, "Nauka", 1986.
5. Kondratyev V. Rate Constants of Gas-Phase Reactions. M., "Nauka", 1970, 351 p.
6. Zhdanov V. Rate of Chemical Reaction. Novosibirsk: Nauka, 1986, 100p.
7. Pikaev A., Kabakchi S. Reactivity of Primary Products of Water Radiolysis. M.: Energoatomizdat, 1982, 199p.
8. Ed. Palm V. Tables of Rate Constants and Equilibrium of Heterolytic Organic Compounds. M.: VINITI, 1975, 431p.
9. Denisov E. Rate Constants of Homolytic Liquid-Phase Reactions. M.: "Nauka", 1971, 711p.